J Mater Sci (2007) 42:9469–9475
DOI 10.1007/s10853-006-0702-7

Cone crack initiation induced by contact from cylindrical punch

Y. J. Xie · D. A. Hills · X. Z. Hu

Received: 5 February 2006 / Accepted: 24 July 2006 / Published online: 27 July 2007

Abstract The critical load for cone crack initiation in a brittle material indented by a rigid cylindrical punch is related to the fracture toughness of the material and the punch radius through the classical energy principles. The strain energy required to form an embryo cone crack on a flaw-free surface adjacent to the punch edge is formulated, from which the critical load for cone cracking is then determined. The present analysis shows that the stress singularity close to the sharp contact edge is akin to that a sharp crack tip. The results in this study can be used to set up a simple and practical technique for evaluating some strength-related properties of brittle materials such as the fracture toughness.

Introduction

It has been well documented that if a rigid spherical or cylindrical body is pressed into a large flat glass block, a cone crack will form suddenly at a characteristic load [1]. This beautiful crack, as they have come to be known, has been a rich and productive topic of research over the post century, and remains so because of its relevance to contact failures of materials such as bi- and tri-layer structures with brittle and coatings in many recent bio-materials applications.

It has been proven to be difficult to establish a satisfactory analytical solution to quantitatively describe the formation of an embryo and growth of a cone crack, which are the two basic contact damage problems. The first one concerns sudden cracking on the flaw-free surface. The second one concerns the initiation and growth of the pre-existing cone crack. The mechanism of cone crack initiation and propagation is relative well understood by Sneddon [2] stress tensor and fracture mechanics [3]. Up to now, nearly all papers on surface contact damage were concentrated on the cone crack initiation and propagation such as the references [4–8]. The present work will focus on sudden surface cracking on the flaw-free surface of a brittle solid.

There have been many indentation tests performed over the years, most using a spherical indenter while some using a square-ended cylindrical indenter, such as the well-known tests conducted by Roesler [9]. The Hertzian contact test using a spherical indenter, despite its simplicity, does have some drawbacks. For instance, the contact area increases with an increasing indentation load, and therefore the surface trace of an initiated cone crack can be easily engulfed by the expanding contact circle, causing secondary fracture because of the indentation load acting over the cone crack and the supporting material underneath [3]. Furthermore, stress trajectories move as the radius of contact increases, making any analytical attempt untraceable. As recognized by Roesler [9], a cylindrical punch with a flat end and sharp edge would not have those problems, so analytically this geometry with a constant

Y. J. Xie (✉)
Department of Mechanical Engineering, Liaoning University of Petroleum & Chemical Technology, Fushun 113001 LN, P.R. China
e-mail: yjxie@lnpu.edu.cn

D. A. Hills
Department of Engineering Science, Oxford University, Parks Road, Oxford OX1 3PJ, UK

X. Z. Hu
School of Mechanical Engineering, The Western University of Australia, Perth, WA 6009, Australia

contact radius would be a preferred choice for cone crack modeling.

Another important feature of a square-ended cylindrical punch is that there is a pre-existing stress singularity present at the edge of contact, which does not exist if a spherical indenter is used. This feature is more in line with the classic concept of stress intensity factor commonly dealt with in fracture mechanics. The present study will show such a stress singularity plays a significant role in the cone crack formation, and provides a close form solution similar to that of a sharp crack. The contact analysis developed in this study is then used to predict cracking along the contact edge due to the stress singularity and its angle relative to the contact surface. This mechanism relevant to the cone crack embryo or cracking along the contact edge on the flaw-free surface is unique as the critical load for cone crack embryo will be controlled by the singular stress field associated with the punch edge. In other words, the critical load itself can be inferred from the conventionally defined fracture toughness. It should be emphasized that this approach would apply only for a completely flaw-free surface so that the stress singularity is solely defined by the contact.

Contact problem

In the present study, we consider the case of a frictionless cylindrical punch pressing onto a flat surface of glass plate or an ideal brittle material, as shown in Fig. 1. It is assumed that the punch has a perfect sharp corner and is rigid in comparison with the stiffness of the elastic material under indentation. In this case, the deformation can only occur within the glass body so that the half-space contact theory is valid. Under the simplified assumption of a rigid frictionless punch, the contact problem may then be solved analytically in a close form solution so that the stress state relevant to the cone crack formation can be evaluated. In particular, we are going to show that, in the neighborhood of the corner rim of the rigid and perfectly sharp punch, the local state of stress varies in an identical manner to that ahead of a crack tip.

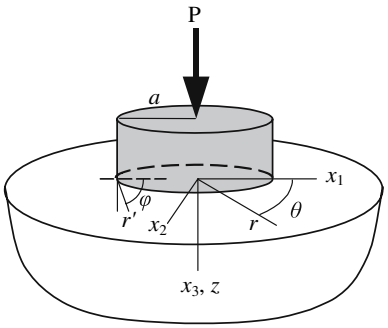

Fig. 1 Schematic representation of the contact between a rigid cylindrical punch and an elastic half space

The indentation geometry considered is illustrated in Fig. 1. The indenter is a cylindrical rigid flat punch of diameter $2a$ and is pressed onto a flat surface of glass plate. Using the cylindrical coordinate system r, θ, z, shown in Fig. 1, Sneddon [2] found the stress field, as given by

$$\begin{pmatrix} \sigma_{zz} \\ \sigma_{rz} \\ \sigma_{\theta\theta} \\ \sigma_{rr}+\sigma_{\theta\theta} \end{pmatrix} = -\frac{4\mu(\lambda+\mu)h}{(\lambda+2\mu)\pi a} \begin{pmatrix} I_1^0+\zeta I_2^0 \\ \zeta I_2^1 \\ \lambda I_0^1+(I_0^1-\frac{\lambda+\mu}{\mu}\zeta I_2^1)/\rho \\ (2\lambda+\mu)I_1^0-(\lambda+\mu)\zeta I_2^0 \end{pmatrix}, \tag{1}$$

where λ and μ are Lame's elastic constants, $\rho = r/a$ and $\zeta = z/a$ are normalized coordinates, and h is the indentation depth related to the applied normal force, P, by

$$P = \frac{8\mu(\lambda+\mu)}{\lambda+2\mu}ah. \tag{2}$$

The functions I_1^0, I_2^1, I_2^0, I_0^1 used in Eq. 1 are given by

$$I_1^0 = R^{-1/2}\sin\frac{\omega}{2}, \quad I_2^1 = \rho R^{-3/2}\sin\frac{3\omega}{2},$$
$$I_2^0 = r^* R^{-3/2}\sin\left(\frac{3\omega}{2}-\Omega\right), \quad I_0^1 = \frac{1}{\rho}\left(1-R^{1/2}\sin\frac{\omega}{2}\right) \tag{3}$$

where the transformed normalized coordinates are

$$r^{*2} = 1+\zeta^2,^2 = \left(\rho^2+\zeta^2-1\right)^2+4\zeta^2, \quad \tan\Omega = 1/\zeta,$$
$$\tan\omega = 2\zeta/\left(\rho^2+\zeta^2-1\right) \tag{4}$$

Taking the asymptotic limit (see Fig. 1), $r' \to 0$ at the surface [10] ($\zeta \to (r'/a)\sin\varphi$) and evaluate the state of stress adjacent to the contact edge, so that $r \to a$, $z \to 0$. Do this by $\rho \to 1-(r'/a)\cos\varphi$. We obtain $\Omega \to \pi/2 - (r'/a)\sin\varphi$, $\omega \to \pi-\varphi$, $r^* = 1$, $R \to 2(r'/a)(1-(a/r')\cos\varphi)$. Then,

$$\begin{pmatrix} \sigma_{zz} \\ \sigma_{rz} \\ \sigma_{rr} \\ \sigma_{\theta\theta} \end{pmatrix} = -\frac{K_I}{\sqrt{2\pi r'}}\cos\frac{\varphi}{2} \begin{pmatrix} 1+\sin\frac{\varphi}{2}\sin\frac{3\varphi}{2} \\ \sin\frac{\varphi}{2}\cos\frac{3\varphi}{2} \\ 1-\sin\frac{\varphi}{2}\sin\frac{3\varphi}{2} \\ 2\nu \end{pmatrix} \tag{5}$$

where

$$K_I = \frac{P}{2a\sqrt{\pi a}}. \tag{6}$$

Interestingly, if the negative sign in Eq. 5 is changed into positive, this result will be the same as that for a

circular semi-infinite crack located along the circumference of a cylindrical rod [11–13] (with an uncracked ligament of radius a) loaded remotely with a normal load P. This finding is important as it shows that the cone crack formation in the current case can be treated as a crack growth problem with a well-defined stress singularity. As shown in Eq. 5, the stress intensity factor K_I is the only parameter controlling the stress field, i.e., there is K-dominant region close to the contact edge, which means that cracking along the contact edge should be controlled by the same mechanism of fracture similar to the Mode I crack. Therefore, the concept of the fracture toughness K_{Ic} should be applicable.

Energy release rates for boundary cracking

This section describes a method for calculating the energy release rate associated with the initiation of a crack from the free boundary. The energy release rate related to a boundary translation has been investigated by Eshelby [14], Sih [15], Budiansky and Rice [16]. Consider a three-dimensional elastostatic boundary value problem with material contained within the surface $S + s$ as shown in Fig. 2, where the portion s of the boundary is traction-free, and external loading is imposed only by tractions on S. Without changing the boundary conditions on S, impose a continuously varying sequence of static solutions, related to the displacements u, given by a time-like parameter t. Details of the procedure can be found in reference [16]. Here, only the final result of energy release rate per unit time, $\partial\Pi/\partial t$, is given, i.e.

$$\frac{\partial \Pi}{\partial t} = \iint_s w v_i m_i \mathrm{d}s, \tag{7}$$

where v_i denotes the '*velocity*' of the points on s and m_i is the outward normal to s.

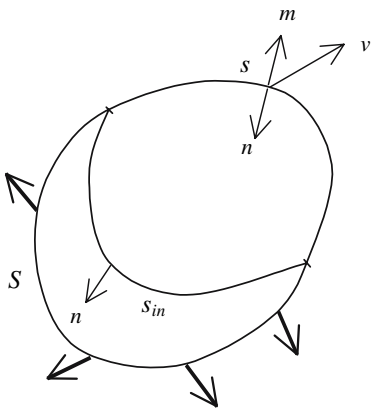

Fig. 2 Three-dimensional deformation fields and integration surface

Let $v_i = e_i = \Delta_i/\Delta$, which corresponds to three components of unit translation, so that $e_1 = \cos\alpha$, $e_2 = \cos\beta$ and $e_2 = \cos\gamma$, where α, β, γ are angles between displacement Δ and coordinate axis. Let $n_i = -m_i$ be the unit inward normal on boundary s, which means that the boundary s moves inward. Thus, the energy release rate of boundary translation is given by

$$\bar{G} = -\frac{\partial \Pi}{\partial \Delta} = \iint_s w e_i n_i \mathrm{d}s. \tag{8}$$

Now, consider a case of an axisymmetric problem illustrated in Fig. 3. Let all the points on the boundary s move in the same direction and with the same value, Δ, in the plane of (z, r) expressed on the cylindrical coordinates. Then $e_r = \sin\beta$, $e_z = \cos\beta$ $e_\theta = 0$ (see Fig. 3). Combining these results with the conservation law J_i [14–16] expressed in the form of cylindrical coordinates [17], the energy release rate defined by Eq. 8 can be rearranged as follows:

$$\bar{G} = J_r \sin\beta + J_z \cos\beta, \tag{9}$$

where

$$J_r = \iint_s \left(w n_r - T_i u_{i,r}\right)\mathrm{d}s = \iint_{s_{\mathrm{in}}} \left(w n_r - T_i u_{i,r}\right)\mathrm{d}s, \tag{10}$$

$$J_z = \iint_s \left(w n_z - T_i u_{i,z}\right)\mathrm{d}s = \iint_{s_{\mathrm{in}}} \left(w n_z - T_i u_{i,z}\right)\mathrm{d}s. \tag{11}$$

Here s_{in} is any integration surface within the space enclosed by boundary $S + s$, with the condition that $s_{\mathrm{in}} + s$ forms a closed surface. β is the semi-angle of cone cracking. The physical meaning of Eq. 10 is the energy release rate for unit translation of boundary s in direction r, and Eq. 11 in direction z.

From the geometrical point of view, boundary cracking or crack initiation, whether it occurs at a crack tip, a notch corner or on a general boundary, can be considered as a

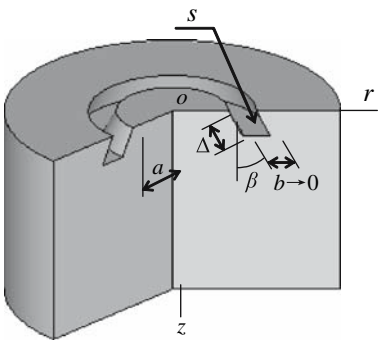

Fig. 3 Model of boundary cone cracking

boundary translation in some direction, with the limit $b \to 0$, as shown in Fig. 3. Then, the energy release rate of boundary cracking $\tilde{G}$ or the energy release rate due to crack embryo can be defined as

$$\tilde{G} = \bar{G}|_{b\to 0} = (J_r)|_{b\to 0} \sin\beta + (J_z)|_{b\to 0} \cos\beta, \tag{12}$$

where $(J_r)|_{b\to 0}$ denotes the driving force of the boundary cracking in direction r and $(J_z)|_{b\to 0}$ denotes the driving force in direction z, when the required limits exist. Since $b \to 0$ and $\Delta \to 0$ mean the crack embryo or boundary cracking, Eq. 12 represents the energy release rate for boundary cracking in direction β.

We turn, first, to determine the critical condition for the formation of a *plane crack* through evaluation of the critical strain energy release rate, $\tilde{G}_c$, by these principles. For a two dimensional crack subjected to both remote opening (Mode I) and shear type (Mode II) loading as depicted in Fig. 4, the counterpart of Eq. 12 becomes:

$$\tilde{G}^{\circ} = J_1 \cos\alpha + J_2 \sin\alpha, \tag{13}$$

which means the energy release rate of boundary cracking in any direction α with unit thickness; and the integrals J_i around the crack tip within the K-dominant region, in terms of the stress intensity factors K_I and K_{II}, are

$$J_1 = \frac{1-\mu^2}{E}\left(K_I^2 + K_{II}^2\right), \quad \text{(plane strain)} \tag{14}$$

$$J_2 = -\frac{1-\mu^2}{E} K_I K_{II}, \quad \text{(plane strain)} \tag{15}$$

From Eq. 13 the strain energy release rate of the crack tip along any general angle α can be expressed as

$$\tilde{G}^{\circ} = \left(\sqrt{J_1^2 + J_2^2}\right) \cos(\alpha - \alpha_{\circ}), \tag{16}$$

where

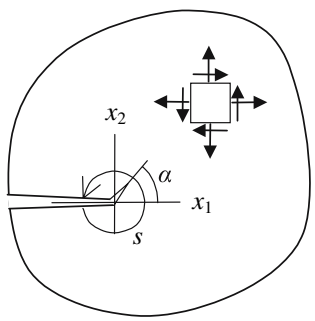

Fig. 4 Crack and cracking angle

$$\alpha_{\circ} = \tan^{-1}\left(-\frac{2K_I K_{II}}{K_I^2 + K_{II}^2}\right). \tag{17}$$

The strain energy release rate may be maximized by setting $\frac{\partial \tilde{G}^{\circ}}{\partial \alpha} = 0$, which gives $\sin(\bar{\alpha} - \alpha_{\circ}) = 0$. The optimum angle $\bar{\alpha}$ at which $\tilde{G}^{\circ}$ takes its maximum value is then given by

$$\bar{\alpha} = \alpha_{\circ}, \tag{18}$$

and the maximum value of the energy release rate is

$$\tilde{G}^{\circ}_{\max} = \sqrt{J_1^2 + J_2^2}. \tag{19}$$

These results are identical with those derived by Cherepanov [18].

For homogenous and isotropic brittle materials Griffith's criterion [19] states that the crack will extend when the critical value $\tilde{G}_c^{\circ}$ is reached [18], i.e.,

$$\tilde{G}^{c}_{\max} = \tilde{G}_c^{\circ} \tag{20}$$

For a standard specimen subjected to Mode I loading, $\tilde{G}^{\circ}_{\max} = J_1$ and $\tilde{G}_c^{\circ}$ can be calibrated from

$$\tilde{G}_c^{\circ} = J_{IC} = K_{IC}^2\left(1-\mu^2\right)/E, \tag{21}$$

where K_{IC} is the fracture toughness.

Turn, now to the axisymmetric penny shaped crack. The critical value of Eq. 12 becomes

$$\tilde{G}_c = 2\pi a \tilde{G}_c^{\circ} = 2\pi a K_{IC}^2\left(1-\mu^2\right)/E, \tag{22}$$

Application to contact between cylindrical rigid punch and friction less half-space

The procedure described above has been applied to the bearing contact described in "Contact problem". For the same configuration, Roesler's [9, 20] experimental results indicated that the cone crack initiated just outside the contact circle. Then, the s in Eqs. 10 and 11 and Fig. 3 is taken as $z = 0$, $a^+ \leq r \leq a^+ + b$ and $b \to 0$ within the K-dominant region as shown in Figs. 5 and 6. This is an important step for boundary cracking analysis because the strain energy needed to start a cone crack at the perimeter of the cylindrical contact punch can be found, by evaluating the contour integrals along the surface shown in Figs. 5 and 6.

First, the value of J_r was found. Let $s_{\text{in}} = s_1 + s_2$ in Eq. 10, where $s + s_1 + s_2$ forms a closed curve; and let $b \to 0$ as shown in Fig. 5a. Adjacent to the perimeter of the punch, J_r can be expressed by

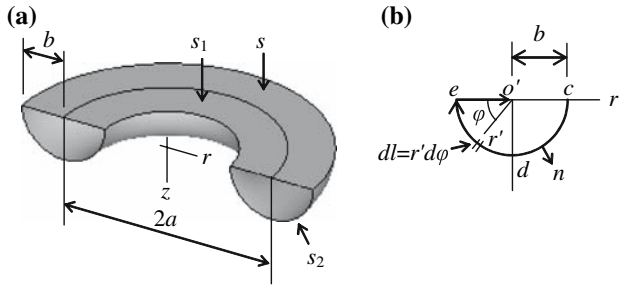

Fig. 5 Integration surface for calculation of J_r, (**a**) half symmetric integration surface, (**b**) integration path in (r, z) plane

$$J_r = \iint_{s_{\text{in}}} \left(wn_r - T_i u_{i,r}\right) \mathrm{d}\Omega = \iint_{s_1} \left(wn_r - T_i u_{i,r}\right) \mathrm{d}\Omega + \iint_{s_2} \left(wn_r - T_i u_{i,r}\right) \mathrm{d}\Omega. \tag{23}$$

From this it is not difficult to prove that

$$\iint_{s_1} \left(wn_r - T_i u_{i,r}\right) \mathrm{d}\Omega = 0 \tag{24}$$

and

$$\iint_{s_2} \left(wn_r - T_i u_{i,r}\right) \mathrm{d}\Omega = 2\pi \int_{s_{cde}} \left(wn_r - T_i u_{i,r}\right) (a - b\cos\varphi)\mathrm{d}l \overset{b/a\to 0}{=} \frac{a\pi(1-\mu^2)K_I^2}{E}. \tag{25}$$

Thus, Eq. 23 becomes

$$J_r|_{b\to 0} = \frac{a\pi(1-\mu^2)K_I^2}{E}. \tag{26}$$

We now evaluate J_z. Within the K-dominant region, let $s_{\text{in}} = s_1 + s_2$in Eq. 11 and take the limit $b \to 0$ as shown in Fig. 6. Under these conditions, the J_z integral becomes

$$J_z = \iint_{s_{\text{in}}} \left(wn_z - T_i u_{i,z}\right) \mathrm{d}\Omega = \iint_{s_1} \left(wn_z - T_i u_{i,z}\right) \mathrm{d}\Omega + \iint_{s_2} \left(wn_z - T_i u_{i,z}\right) \mathrm{d}\Omega. \tag{27}$$

Note that s_1 is a cylindrical shell and s_2 is shaped by rotating a quarter of a circle around axis z. Along the surfaces s_1 and s_2, shown in Fig. 6a and b, the following integration results can be obtained from Xie [21–24]

$$\iint_{s_1} \left(wn_z - T_i u_{i,z}\right) \mathrm{d}\Omega = 0 \tag{28}$$

and

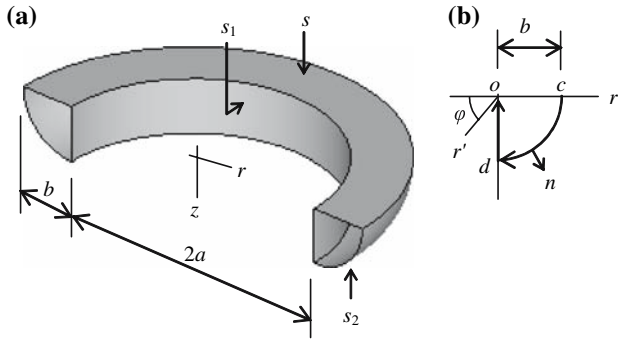

Fig. 6 Integration surfaces for calculation of J_z, (**a**) half symmetric integration surface, (**b**) integration path in (r, z) plane

$$\iint_{s_2} \left(wn_z - T_i u_{i,z}\right) \mathrm{d}\Omega = 2\pi \int_{s_{cd}} \left(wn_z - T_i u_{i,z}\right) (a - b\cos\varphi)\mathrm{d}l \overset{b/a\to 0}{=} \frac{a(1-\mu^2)K_I^2}{E} \tag{29}$$

Thus, Eq. 27 now becomes

$$J_z|_{b\to 0} = \frac{a(1-\mu^2)K_I^2}{E}. \tag{30}$$

From Eq. 12, the total energy release rate of boundary cracking at any angle β can be found as

$$\tilde{G} = (J_r)|_{b\to 0}\sin\beta + (J_z)|_{b\to 0}\cos\beta = \frac{a(1-\mu^2)K_I^2\sqrt{1+\pi^2}}{E}\cos(\beta - \beta_\circ) \tag{31}$$

where

$$\beta_\circ = \tan^{-1}\pi = 72.34 \text{ deg}. \tag{32}$$

The energy release rate is now maximized with respect to $\bar{\beta}$ by the condition $\frac{\mathrm{d}\tilde{G}}{\mathrm{d}\beta} = 0$, i.e., $\sin\left(\bar{\beta} - \beta_\circ\right) = 0$, which gives

$$\bar{\beta} = \beta_\circ = 72.34 \text{ deg}. \tag{33}$$

where $\bar{\beta}$ is the theoretically predicted cracking angle at which $\tilde{G}$ exhibits a maximum value, and is given by

$$\tilde{G}_{\max} = \frac{a(1-\mu^2)K_I^2\sqrt{1+\pi^2}}{E}. \tag{34}$$

The most widely used fracture criterion is Griffith's [19] theory. The energy criterion of Griffith yields, in principle, a minimum critical load for failure. Thus, according to Eqs. 22 and 34, the critical condition for cracking along the flaw-free boundary becomes

$$\tilde{G}_{\max} = 2\pi a\tilde{G}_c'. \tag{35}$$

where $\tilde{G}_c'$ is the critical energy release rate per length of boundary for compressive singular stress fields, which should be determined by experimental method similar to J_{IC}. Additionally, from Eqs. 6, 34, 35, the Eq. 35 can be written as

$$K_I = \frac{P}{2a\sqrt{\pi a}} = \frac{\sqrt{2\pi}}{(\pi^2+1)^{1/4}} K'_{IC}, \tag{36}$$

where $K'_{IC} = \sqrt{E\tilde{G}'_{IC}/(1-\mu^2)}$. Equation 36 gives a K-based critical condition, which defines a relationship between the stress intensity factor and fracture toughness for boundary cracking in a half space. It should be emphasized that, in the above analysis, the stress intensity factor used is defined by Eq. 6, which is the parameter controlling the stress singularity at the punch perimeter. Instead of the crack size in a normal stress intensity factor relation, the radius of the punch is the length parameter, which is a geometrically defined pre-existing known quantity. Equation 36 can be used to calculate the critical load to induce the cone crack formation along the contact boundary.

$$P_c = \frac{\pi(2a)^{3/2}}{(\pi^2+1)^{1/4}} K'_{IC}. \tag{37}$$

Alternatively, we can determine the critical punch radius for a given contact force, P, as

$$a_c = \frac{(1+\pi^2)^{1/6}}{2}\left(\frac{P}{\pi K'_{IC}}\right)^{2/3}. \tag{38}$$

The remarkable feature of this calculation is that the fracture load can be evaluated in a simple close form solution, without the need to know the pre-existing flaw size distribution.

In fact, K'_{IC} related to the compressive Mode I singular stress fields should be different from the classical K_{IC} for tensile singular stress fields. With these reservations in mind we postulate with recourse to Eqs. 22, 35, 36, i.e., $K_{IC} = K'_{IC}$. Explicitly, for glass the value of the fracture toughness is usually taken to be about 0.7 MPa $\sqrt{\text{m}}$, and hence the value of the predicted fracture load as a function of the contact radius a is as shown in Fig. 7.

Equation 33 indicates that $\bar{\beta}$ is independent of the indenter diameter. This conclusion is supported by Roesler's experimental results [9]. In his classic experiments, Roesler found that the crack cone semi-angle can given by $\bar{\beta}_R = 68.5$ deg ± 1 deg. According to present theory, the theoretical predicted crack cone semi-angle is $\bar{\beta} = 72.34$ deg, from the Eq. 33. The relative error is 5.3%.

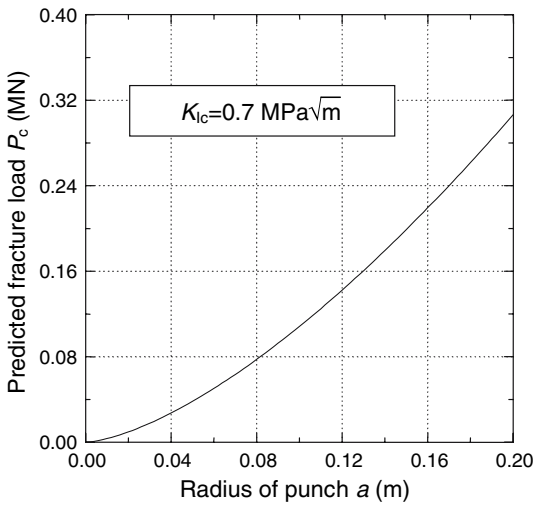

Fig. 7 Predicted fracture load, a function of contact radius, for a material with the fracture toughness shown

Conclusions

Different from indentation with a spherical indenter, there is a pre-existing stress singularity present at the contact edge of a rigid cylindrical punch. The present study has established the cone crack formation condition analytically by linking the stress singularity to a K-dominant stress field, which is similar to the Mode-I crack extension. This represents a new possible mechanism for cone crack formation on a flaw-free surface of a brittle material.

Using the conservation law, the energy release rate of cracking along the contact edge, or cone crack initiation, in any direction has been defined for three-dimensional axisymmetric solids. The problem of three-dimensional contact between a rigid cylindrical punch and a flaw-free brittle material has been investigated by using the proposed method. The cracking angle and critical load for initial failure of the brittle material have been derived. The analysis predicts that the semi-angle of the cone cracking is independent of the indenter diameter, and this angle is close to the experimental result by Roesler [9].

Unlike the traditional method for testing fracture toughness, the current study shows that the singular stress field and the K-dominant region can be induced by indentation on a flaw-free surface, which imply the potential possibility to set up a very simple and practical technique for evaluating some strength-related properties of materials such as the fracture toughness using specimens without macro-pre-existing cracks. It is realized that the condition of a rigid cylindrical punch with a perfectly sharp corner is highly idealized, which may not be satisfied in an experiment. Although some error is expected, the general relation proven by Eq. 37 should hold.

References

1. Frank FC, Lawn BR (1967) Proc R Soc 299:291
2. Sneddon IN (1946) Camb Philos Soc 42:29
3. Mouginot R, Maugis D (1985) J Mater Sci 20:4354
4. Kocer C, Collins RE (1998) J Am Soc 81(7):1736
5. Fischer-Cripps AC (1997) J Mater Sci 32:1277
6. Warren R (1978) Acta Metall 26:1759
7. Fischer-Cripps AC, Coolins RE (1994) J Mater Sci 29:2216
8. Wang R, Katsube N, Seghi RR, Rokhlin SI (2003) J Mater Sci 38:1589
9. Roesler FC (1956) Proc R Soc 69:981
10. Giannakopoulos AE, Lindley TC, Suresh S (1998) Acta Mater 46:2955
11. Tada H, Paris PC, Irwin GR (1973) Stress analysis of cracks handbook. Dil Rsearch Corporation, Hellertown
12. Rooke DPG, Cartwright DJ (1976) Compendium of stress intensity factors. Her Majesty's Stationary Office, London
13. Murakami Y (1987) Stress intensity factors Handbook. Pergammon Press, New York
14. Eshelby JD (1951) Phil Trans R Soc Lond Ser A 244:87
15. Sih GC (1969) Inelastic behavior of solids. Mc-Graw-Hill Book, Co., New York, p 607
16. Budiansky B, Rice JR (1973) ASME J Appl Mech 40:201
17. Knowles JK, Sternberh E (1972) Arch Ration Mech Anal 44(3):187
18. Cherepanov GP (1979) Mechanics of brittle fracture. Publish House "Nuaka", Moscow, 1974, English trans published by McGraw-Hill International Book Co., New York, p. 266
19. Griffith AA (1921) Phil Trans R Soc Lond A221:163
20. Lawn BR, Wilshaw TR (1975) Fracture of brittle solids. Cambridge University Press, Cambridge, p. 63
21. Xie YJ, Xu H, Li PN (1998) Theor Appl Fract Mech 29:195
22. Xie YJ (1998) Int J Pres Ves Pip 75:865
23. Xie YJ, Zhang X, Wang XH (2001) Int J Solids Struct 38:6953
24. Xie YJ (2000) Int J Solids Struct 37:5189